Structural insights into the semiquinone form of human Cytochrome P450 reductase by DEER distance measurements between a native flavin and a spin labelled non-canonical amino acid

Maxime Bizet, Deborah Byrne, Frédéric Biaso, Guillaume Gerbaud, Emilien Etienne, Giuseppina B Briola, Bruno Guigliarelli, Philippe Urban, Pierre Dorlet, Tamas Kalai, et al.

RESEARCH ARTICLE

Structural insights into the semiquinone form of human Cytochrome P450 reductase by DEER distance measurements between a native flavin and a spin labelled non-canonical amino acid

Maxime Bizet,[a] Deborah Byrne,[b] Frédéric Biaso,[a] Guillaume Gerbaud,[a] Emilien Etienne,[a] Giuseppina Briola,[a] Bruno Guigliarelli,[a] Philippe Urban,[c] Pierre Dorlet,[a] Tamas Kalai,[d] Gilles Truan[c] and Marlène Martinho*[a]

[a] M. Bizet, Dr. F. Biaso, Dr. G. Gerbaud, Dr. E. Etienne, G. Briola, Prof. B. Guigliarelli, Dr. P. Dorlet and Dr. M. Martinho
Aix Marseille Univ, CNRS, Bioénergétique et Ingénierie des Protéines, IMM, Marseille (France)
E-mail : mmartinho@imm.cnrs.fr

[b] Dr. D. Byrne
Protein Expression Facility
Aix Marseille Univ, CNRS, IMM
13402 Marseille (France)

[c] Dr. P. Urban, Dr. G. Truan
TBI, Université de Toulouse, CNRS, INRAE, INSA, Toulouse, France

[d] Prof. T. Kalai
Department of Organic and Medicinal Chemistry, Faculty of Pharmacy
University of Pécs
H-7602 7624 Pécs, PO Box 99 Szigeti st. 12, Hungary

Supporting information for this article is given via a link at the end of the document.

Abstract: The flavoprotein Cytochrome P450 reductase (CPR) is the unique electron pathway from NADPH to Cytochrome P450 (CYPs). The conformational dynamics of human CPR in solution, which involves transitions from a "locked/closed" to an "unlocked/open" state, is crucial for electron transfer. To date, however, the factors guiding these changes remain unknown. By Site-Directed Spin Labelling coupled to Electron Paramagnetic Resonance spectroscopy, we have incorporated a non-canonical amino acid onto the flavin mononucleotide (FMN) and flavin adenine dinucleotide (FAD) domains of soluble human CPR, and labelled it with a specific nitroxide spin probe. Taking advantage of the endogenous FMN cofactor, we successfully measured for the first time, the distance distribution by DEER between the semiquinone state $FMNH^{\bullet}$ and the nitroxide. The DEER data revealed a salt concentration-dependent distance distribution, evidence of an "open" CPR conformation at high salt concentrations exceeding previous reports. We also conducted molecular dynamics simulations which unveiled a diverse ensemble of conformations for the “open” semiquinone state of the CPR at high salt concentration. This study unravels the conformational landscape of the one electron reduced state of CPR, which had never been studied before.

Introduction

Microsomal cytochrome P450s (CYPs) occupy a pivotal role in human drug (70% of commonly prescribed drugs), fatty acid and steroid metabolisms.[1,2] To perform their functions, CYPs require electrons, which are provided by a specific flavoprotein, the NADPH cytochrome P450 reductase (CPR). CPR is located on the cytoplasmic side of the endoplasmic reticulum (ER). The electron transfer (ET) process involves a nicotinamide adenine dinucleotide phosphate (NADPH) co-factor, which provides a hydride to CPR. Electrons then transit via CPR’s flavin cofactors (Figure 1A), from flavin adenine dinucleotide (FAD) to flavin mononucleotide (FMN), reaching its final electron acceptor, the heme iron of CYPs. Molecular ET requires extensive domain movements, transitioning between so-called “locked/closed” (for intra-ET “FAD to FMN”) and “unlocked/open” (for inter-ET “FMN to the heme iron of CYPs”) states of CPR.[3] The conformational equilibrium within *Homo sapiens* CPR has been studied through both spectroscopic and structural approaches, essentially on mutated or truncated proteins.[3–7] Undoubtedly, these studies highlight the immense significance of the connection between dynamics and function, as domain movement can exert precise control over the efficiency of ET and activities of CYPs, and consequently have a substantial impact on CYP-mediated drug metabolism.[7,8] Crystal structures of *Rattus norvegicus* soluble CPR are available in two distinct states: the “locked/closed” (pdb. 1amo, Δ64) and partially “unlocked/open” (pdb. 3ES9, ΔTGEE), the last one being non-functional. In these structures, the FMN to FAD N5-N5 distances span a range from 13 to 32 Å respectively. On the other hand, crystal structures have been reported for *Homo sapiens wt* CPR (Figure 1B), captured in its “locked/closed”

state, with a FMN to FAD N5-N5 distance of 13 Å (pdb. 5FA6 for Δ66 and 3QE2 for Δ66-P228L/A503V). A highly open state, derived from a chimeric *Saccharomyces cerevisiae*/*Homo sapiens* construct, and featuring a FAD-FMN N5-N5 distance of 84 Å, has also been reported (Figure S1, pdb. 3FJO).[9] The existence of these closed/open states was the foundation for a two-state equilibrium model hypothesis. Still, the factors governing the presence of CPR multiple conformations in solution, and the switch between them, remain a subject of ongoing debate.[2,10] Indeed, it has been demonstrated that factors such as flavin redox states, ionic strength[6] and specific mutations on CPR play important roles in the conformational equilibrium modulation.[2] Nevertheless, molecular data on functional *wt Homo sapiens* CPR in solution related to its dynamics are still missing, especially in presence of CYPs isoforms. Here we demonstrate the power of Site-Directed Spin Labelling coupled to Electron Paramagnetic Resonance (SDSL-EPR) spectroscopy to unravel the conformational landscape of "locked/closed" and "unlocked/open" of soluble and functional *Homo sapiens* CPR in solution.

SDSL-EPR and DEER (Double Electron-Electron Resonance) stand as a robust method for acquiring precise dynamic and structural insights into both soluble and membrane proteins. This approach relies on the strategic introduction of a nitroxide label, typically on cysteine residues, at a specific site.[11–13] When two such labels are present on the protein, DEER reports on spin-spin dipolar interaction, providing access to distance distributions in a $1/r^3$ manner.[13–15] SDSL-EPR investigations of membrane-bound CPR have previously been conducted by incorporating spin probes on surface exposed cysteine residues. However, these chemical modifications proved detrimental to the activity of the protein, especially in the case of C629 (numbering based on the NCBI Reference Sequence NP_001382342) given its essential role.[16,17] Cysteines are often implicated in catalytic or binding sites, and therefore not the optimal choice for probe labelling. To overcome this biological obstacle, a valuable alternative lies in the bio-orthogonal incorporation of non-canonical amino acids (ncaa) for subsequent labelling with specific nitroxide labels.[18–23] Indeed, recent years have seen the development of bio-orthogonal approaches for biophysical studies.[7] These include SDSL-EPR methods that utilize labels such as i) nitroxide reactive to ncaa,[24,25] ii) triarylmethyl radicals,[26] iii) metal centres like Gd^{3+},[27] Cu^{2+},[28] Mn^{3+}.[29,30] In the case of flavoproteins such as CPR, the flavin can be used to an advantage thanks to its possible semi-quinone (sq) state. Indeed, the stabilization of this sq intermediate, and subsequent labelling of the protein, enables us to accurately measure the distances between said sq and nitroxide sites. In this case, the flavin radical serves as a tightly bound, inherent paramagnetic cofactor. Indeed, the localized spin density distribution within flavin radicals (C(4a) and N(5), figure 1C) makes the DEER based approach valuable to investigate conformational changes in flavoproteins.[31,32] While a handful of DEER data have been previously reported to measure flavin-to-flavin[33–36] or flavin-to-nitroxide distances,[37,38] none of these studies have employed a ncaa. As for CPR, only a single DEER distance measurement between the two sq species, namely $FADH^{\bullet}$-to-$FMNH^{\bullet}$, has been reported to date.[34]

In this study, we have successfully investigated the dynamics and conformational changes of the one electron reduced soluble form of human CPR by incorporating a *p*-azidophenylalanine (*p*AzPhe) amino acid at selected strategic positions and subsequent specific nitroxide labelling. DEER experiments on sq/nitroxide pairs on CPR, and molecular dynamics (MD) studies, have been conducted proving the existence of two main states in solution.

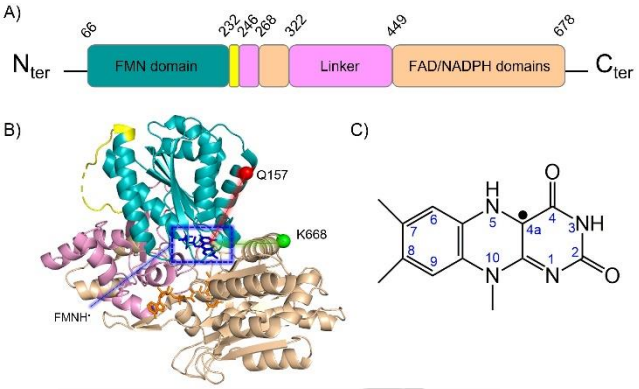

Figure 1. A) Schematic representation of soluble *Homo sapiens* CPR organization and B) "Locked/closed" state crystal structure of soluble *Homo sapiens* CPR (pdb. 5fa6) with Q157 and K668 residues for labelling highlighted as red and green spheres respectively. The FAD and FMN domains are represented in brown and cyan ribbons respectively, FAD and FMN co-factors are shown as sticks in orange and dark blue, linker is shown as light pink ribbon, the flexible loop is shown in yellow. Red and green lines represent distances between $FMNH^{\bullet}$ and the label at positions Q157 and K668, respectively ; blue rectangle highlights the $FMNH^{\bullet}$ species. C) Chemical structure and IUPAB numbering of the isoalloxazine ring of FMN semi-quinone state.

Results and Discussion

Incorporating non-canonical amino acids in soluble CPR and labelling

Two individual *Homo sapiens* soluble CPR (His-Tag-Δ61 *wt*, numbering based on the NCBI Reference Sequence NP_001382342, see SI) mutants were designed, expressed and purified. They both contained a *p*AzPhe non-canonical amino acid at surface exposed sites in either two positions: 157 (FMN domain) or 668 (FAD domain), noted hereafter $Q157^{pAzPhe}$ or $K668^{pAzPhe}$ (Figure 1, SI and figures S2 and S3).[7] Each mutant was labelled with HO-4451 (1-Fluoro-N-[(1-oxyl-2,2,5,5-tetramethyl-2,5-dihydro-1H-pyrrol-3-yl)methyl]cyclooct-2-ynecarboxamide) nitroxide label (noted hereafter $Q157^{pAzPhe*}$ or $K668^{pAzPhe*}$, star standing for the label) through Strain-Promoted Azide-Alkyne Cycloaddition (SPAAC) reaction (SI and scheme 1).[19,39,40] Activity assays of $Q157^{pAzPhe}$ or $K668^{pAzPhe}$ mutants and of $Q157^{pAzPhe*}$ or $K668^{pAzPhe*}$ labelled mutants gave activities comparable to that of CPR *wt* and mutants as previously reported in the literature[7,16] (Figure 2), indicating that neither the ncaa incorporation nor its labelling have impacted the ET capacity of CPR. The activity of soluble CPR before and after labelling (WT and mutants) increases as a function of salt concentration in the same manner. This behaviour is consistent with what has already

been reported, showing a maximum of k_{obs} value at 500 mM NaCl.[7,41]

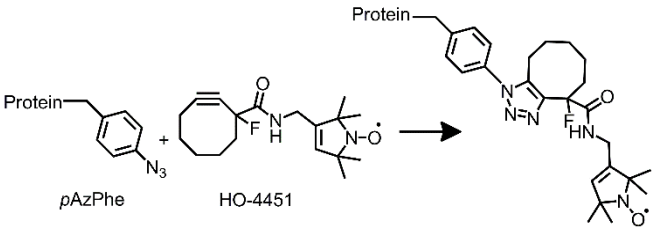

Scheme 1. Labelling SPAAC reaction scheme for *p*AzPhe ncaa with HO-4451 label. Conditions: rt, overnight, into the dark, Tris HCl 20 mM pH 7.4.

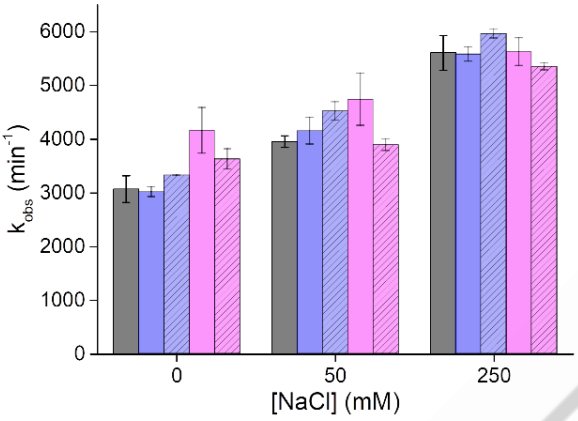

Figure 2. Cytochrome *c* reduction efficiencies determined by the initial velocity k_{obs} of CPR *wt* (grey), Q157^{pAzPhe} (blue) and CPR K668^{pAzPhe} (magenta) as a function of NaCl concentration. Dashed bars correspond to labelled mutants respectively. Error bars represent the standard deviations of triplicates. Temperature: 37°C.

Cw EPR of labelled protein containing ncaas

Continuous wave (cw) EPR spectra of CPR Q157^{pAzPhe*} or K668^{pAzPhe*} (Figure 3A and 3B) were typical of a label in the so-called "intermediate regime of mobility".[42,43] Analysis of the spectra indicated that the label at position Q157 (Figure 3A) experiences a little more constrained environment than at position 668 (Figure 3B), which could be seen by a broader line width of the low- and high-field lines as well as the presence of a supplemental broader component (Figure 3A, arrows). In addition, these results showed that HO-4451 is able to provide structural information on the label environment despite *i)* the size of the ncaa compared to cystein and *ii)* the label larger size compared to the "classical" MTSL (1-oxyl-2,2,5,5-tetramethylpyrroline-3-methylmethanethiosulfonate spin label) label (distance between C_α and the N atom of HO-4451 nitroxide of 14 Å for *p*AzPhe, compared to 8 Å distance in the case of MTSL) (Figure S4).[18]

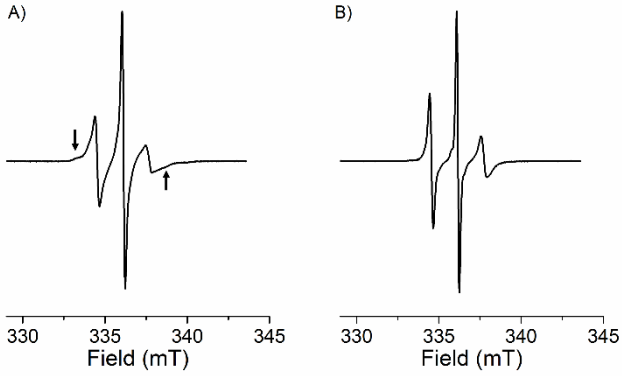

Figure 3. Room temperature cw X-band EPR spectra of labelled *Homo sapiens* CPR mutants A) Q157^{pAzPhe*}, B) K668^{pAzPhe*}. Arrows indicate the broader component in the spectrum. [Q157^{pAzPhe*}] = 516 µM, [K668^{pAzPhe*}] = 417 µM. Buffer: Tris HCl 20 mM pH 7.4. See SI for experimental conditions.

Preparation of FMNH• sq state in labelled CPR and cw EPR characterization

In order to obtain simultaneously a nitroxide site and a paramagnetic flavin co-factor for each mutant, we stabilized the FMNH• sq state by the addition of 1 eq. of NADPH, the physiological electron provider for CPR, to CPR Q157^{pAzPhe*} or K668^{pAzPhe*}. Formation of the sq state was followed by the increase of the electronic absorption band at 620 nm at room temperature, following the same procedure as for the wt protein (Figure S5). An air stabled species FAD/FMNH• (1 electron reduced state)[44–46] was obtained by allowing the solution to oxygenate in air for approximately 10 minutes.

Cw EPR spectra of FMNH•/Q157^{pAzPhe*} and of FMNH•/K668^{pAzPhe*} were recorded in non-saturated conditions in order to quantify each paramagnetic species FMNH• and CPR* (Figure 4 and SI). Note that the EPR spectrum of the flavin radical is quite broad (~30 gauss), which explains the very low amplitude of the FMNH• signal in comparison to the nitroxide one, despite its larger amount. Each experimental spectra was superimposed with those resulting from the linear combination of Q157^{pAzPhe*} or K668^{pAzPhe*} EPR signals (Figure 4A and 4B, spectrum a) with the corresponding FMNH• signal (Figure 4A and 4B, spectrum b). These results indicated the presence of the nitroxide grafted on the protein and the sq species simultaneously (Figures 4A and 4B), in similar sq/nitroxide ratios for both mutants, and consistent with the labelling yield (see SI). Addition of NADPH did not change the nitroxide signals, showing that the label dynamics remained the same in solution for both oxidized and semi-reduced states (Figures 3 and figure 4, spectra a).

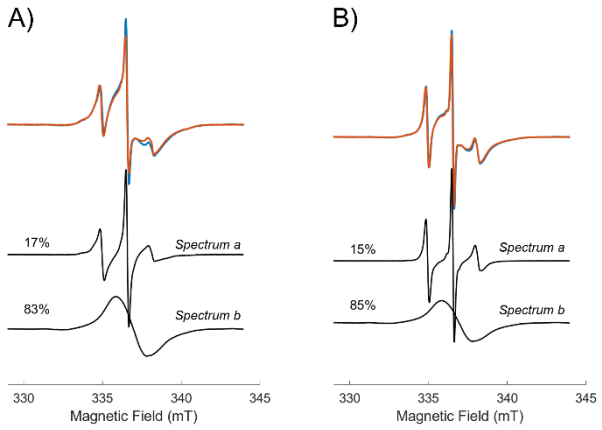

Figure 4. Cw X-band EPR spectra recorded at room temperature of labelled one electron reduced *Homo sapiens* CPR mutants A) FMNH•/Q157^{pAzPhe*} and B) FMNH•/K668^{pAzPhe*}. Orange line: experimental spectrum. Blue line: final spectrum obtained from a linear combination of CPR* alone (spectrum *a*) and FMNH• alone (spectrum *b*) (black lines) with indicated proportions. [Q157^{pAzPhe*}] = 516 µM, [K668^{pAzPhe*}] = 417 µM. Buffer: Tris HCl 20 mM pH 7.4. See SI for experimental conditions.

Ncaa*-FMNH• distance measurements

To provide more information on the domain movement of soluble CPR, we investigated intra-protein distance distribution between the nitroxide spin probe and the FMNH• species. We conducted DEER experiments under varying salt conditions (NaCl at 0, 50 and 250 mM) that favoured the so-called "unlocked/open" state of CPR, depending on the amount of added salt.[3,7,10,11,47] Indeed, ionic strength has been recognized as an *in vitro* experimental condition capable of monitoring the equilibrium between different CPR states. We measured inter-spin distance distributions between the FMNH• sq and the nitroxide label inside the FMN domain (FMNH•/Q157^{pAzPhe*}) and between both the FMN and FAD domains (FMNH•/K668^{pAzPhe*}). For all experiments, the pump (ν_{pump}) and observer ($\nu_{observe}$) frequencies were chosen at the maximum of the FMNH• and nitroxide signals on the echo field sweep (EFS), respectively (Figure S6). The results obtained by DEER experiments are shown in figures 5 and 6 for FMNH•/K668^{pAzPhe*} and FMNH•/Q157^{pAzPhe*} respectively. DEER data showed the presence of a spin-spin dipolar signal for both CPR labelled mutants in the absence of salt (Figures 5A and 6A, blue lines). The observed modulation depth λ values indicated a high amount of FMNH•/CPR^{pAzPhe*} species, and was in agreement with ~50% spin labelling efficiency with our spectrometer configuration (see SI), whatever the labelled position (λ = 0.113 and 0.094 for position Q157 and K668 respectively). In the absence of salt, a restricted ensemble of population centred around a distance distribution of 29 ± 5 Å for FMNH•/K668^{pAzPhe*} and 28 ± 2 Å for FMNH•/Q157^{pAzPhe*} were observed. These values were in agreement with the predicted ones using MMM[48] based on the crystal structure of *Homo sapiens* CPR "locked/closed" state (Figures 5B and 6B, red lines, figure S7). One can note that the width of distance distributions for both mutants probably arise from the presence of label rotamers (Figures S6), as predicted by MMM on a static crystal structure.

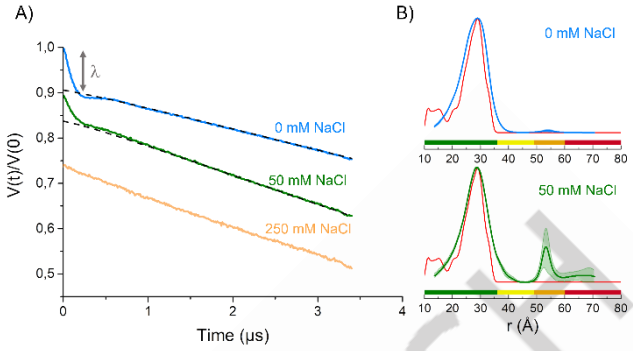

Figure 5. A) Experimental Q-band DEER traces recorded at 60 K for FMNH•/K668^{pAzPhe*} in absence (blue line) or in presence of NaCl 50 mM (green line), 250 mM (orange line). The black dashed lines indicate the baseline used for background correction. DEER traces were shifted vertically for the sake of clarity. B) Distance distributions obtained using the auto-computed mode in DeerAnalysis 2022[49,50] (blue and green lines) and calculated distance distributions for the *Homo sapiens* CPR "locked/closed" (red line) state (pdb. 5FA6 or 3QE2) obtained using the MMM software.[48] For colour code in the x axis, see SI. [K668^{pAzPhe*}] = 90 µM. Buffer: Tris HCl 20 mM pH 7.4, D_2O, 10% v/v d_8-glycerol.

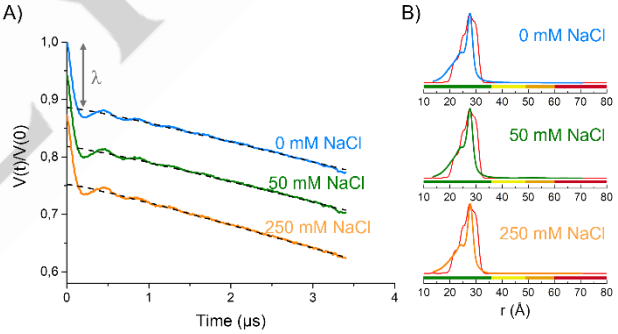

Figure 6. A) Experimental Q-band DEER traces recorded at 60 K for FMNH•/Q157^{pAzPhe*} in absence (blue line) or in presence of NaCl 50 mM (green line), 250 mM (orange line). The black dashed lines indicate the baseline used for background correction. DEER traces were shifted vertically for the sake of clarity. B) Distance distributions obtained using the auto-computed mode in DeerAnalysis 2022[49,50] (blue and green lines) and calculated distance distributions for the *Homo sapiens* CPR "locked/closed" (red line) state (pdb. 5FA6 or 3QE2) obtained using the MMM software.[48] For colour code in the x axis, see SI. [Q157^{pAzPhe*}] = 90 µM. Buffer: Tris HCl 20 mM pH 7.4, D_2O, 10% v/v d_8-glycerol.

Then, we monitored the effect of the ionic strength in order to mimic *in vitro* the opening of the CPR. For FMNH•/Q157^{pAzPhe*}, addition of NaCl did not change the modulation depth (λ = 0.124 and 0.119 for 50 and 250 mM NaCl, respectively), nor the time trace oscillations. Consequently, the distance distributions between the nitroxide and the FMNH• sq remained the same (Figure 6, and figure S9, S10). This result was expected since position Q157 belongs to the FMN domain, and confirmed that *i)*

the FAD remained in its oxidized form, and *ii)* the FMN domain stayed fixed with respect to the rest of the protein (Figure 1).
For FMNH•/K668^{pAzPhe*} the modulation depth decreased by a factor of 2 when adding 50 mM of NaCl (λ = 0.055), and reduced to zero with 250 mM of NaCl. Nevertheless, the EFS signals were comparable for all experiments indicating that the concentration on spin for both FMNH• and the nitroxide were not affected or modified in all three samples with 0, 50 and 250 mM NaCl (Figure S6, S11). The absence of modulation depth and oscillation proved a decrease of the spin-spin dipolar interaction beyond what can be measured with pulsed EPR spectroscopy. This result prevented the extraction of a distance distribution, suggesting an important increase of the distance between the FMNH• sq and the label at position 668. Position 668 being located on the FAD domain, our results highlighted the effect of ionic strength in favouring a more "unlocked/open" state of the CPR in solution, in agreement with previous biophysical studies.[7,8] Nevertheless, our DEER results proved wider open conformations for the specific 1 electron reduced CPR form (FAD/FMNH• state) than what was reported with SAXS data on oxidized or reduced CPR.[6,51] This opening appeared to be reversible as well (Figure S12). Indeed, our results are consistent with MMM calculation performed on the chimeric crystal structure of *Saccharomyces cerevisiae*/*Homo sapiens* CPR construct reported by Aigrain *et al*.[9] In that case, a broad range of distance distributions between FMNH• and position K668 (80 to 100 Å, figure S13C) were obtained, in agreement with the previously mentioned loss of dipolar coupling seen by DEER, and supported by the calculated one (Figure S13A, B). As a comparison, the calculated nitroxide/FMNH• distances for *Rattus norvegicus* in the "unlocked/open" state remained below 40 Å (Figure S14). Overall, our experimental data highlighted the strong effect of ionic strength in modulating the semiquinone CPR conformations between two main "unlocked/open" and "locked/closed" states indicating that this redox state (FAD/FMNH•) does not change the conformational landscape of CPR. For high amount of salt, a highly wide-open conformation was favoured in solution.

Molecular dynamics

To better understand the dynamic behaviour of the *Homo sapiens* CPR, MD simulations were performed on its non-labelled *wt* soluble form. For all simulations, the *wt* enzyme was defined in the air stable state FAD/FMNH•, to match the experiments. Two starting points were created for 400 ns simulations: one in the "locked/closed" state based on the crystal structure of the *Homo sapiens* CPR (pdb code: 3QE2), and one in the "unlocked/open" state inspired by the chimeric *Saccharomyces cerevisiae*/*Homo sapiens* crystal structure (Figure S1, pdb code: 3FJO). For this second conformation, the flavins were initially 84 Å apart (distance N5-N5). Two different salt concentrations were tested for each starting point as well, giving a total of 13 simulations (Table 1). From each MD simulation, the evolution of the distance between the FMNH• (N5) and the K668 C_α was extracted (Figure 7), hereafter named FMNH•/K668.

Table 1 : Number of MD replicas for each condition.

	Starting conformation of CPR	
	Locked/closed	unlocked/open
No salt	3 (green)	4 (red)
NaCl 150mM	3 (dotted brown)	3 (dotted blue)

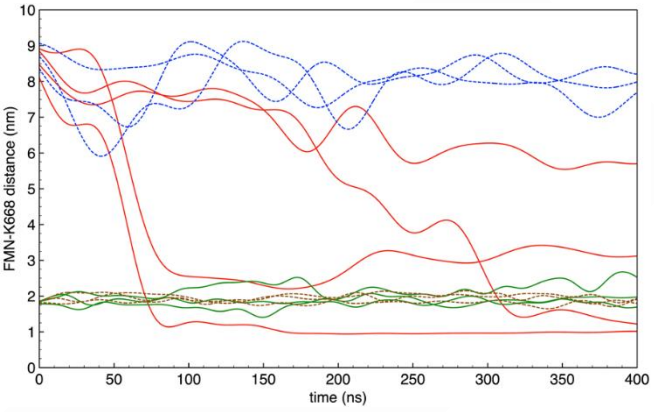

Figure 7. FMNH•/K668 distance evolution for CPR in the FAD/FMNH• redox state. Starting point of the simulation corresponds to the "unlocked/open" state (no salt: red, 150mM NaCl: dotted blue) or "locked/closed" state (no salt: green, 150mM NaCl: dotted brown).

For all simulations starting with a "locked/closed" state (Figure 7, green and dotted brown curves), no large inter-domain movement was calculated over time and the FMNH•/K668 distance therefore remained around 20 Å. This value is in the same range as the experimental one (29 Å, FMNH•/K668^{pAzPhe*}), as we had to take into account the size of the labelled ncaa and the flexibility of this moiety (Figures S4, S7), instead of considering the C_α of the 668-lysine residue. Moreover, these results were in agreement with those reported on the soluble form of the *Rattus norvegicus* CPR, where Iijima *et al.* proposed that the closed form was intrinsically stable and the enzyme predominantly adopted the closed state.[52] The presence of salt did not appear to significantly affect the dynamic behaviour of the semiquinone "locked/closed" state on the timescale of several hundreds of nanoseconds (Figure 7, dotted brown curves).
On the other hand, starting with an "unlocked/open" state (Figure 7, red and dotted blue curves), the dynamic behaviour of the protein was highly dependent on the presence or absence of salt. Indeed, in presence of 150 mM NaCl (dotted blue lines), the two flavin domains (FD) remained highly mobile relative to each other as seen by the broad range of FMNH•/K668 distances, fluctuating between 60 and 90 Å. Nevertheless, the CPR remained overall in an "open" form, reflecting a flexibility and a multiple set of open conformations. In the absence of salt (red lines), the simulations indicated multiple conformation pathways, with a global tendency to a significant decrease of the FMNH•/K668 distance with time. For two of the four simulations, this distance ended up between 10 and 30 Å shortly after 100 ns. In a third simulation, the same result was obtained after a much longer time (300 ns), bringing in

both cases the flavin domains closer to each other in a more "closed" state on this timescale. In the fourth simulation, CPR conformational state stayed in an "open" form all along the simulation time, with a FMNH•/K668 distance above 60 Å. These four different runs suggested once again the effect of the ionic strength in inducing the opening of the two flavin domains and the possibility for the soluble CPR to reach a less "open" state when no salt was present. The time scale of these *in silico* conformational changes were still longer than the ones reported by Šrejber *et al.* where a 10 ns time scale was shown to be sufficient for a spontaneous closing of the structure, the open state being stabilized in presence of a CYP partner.[53]

To have an overall view of the conformations obtained beyond a few hundred nanoseconds, the distribution of the FMNH•/K668 distance obtained using the data for the last 200 ns is presented in figure 8. After 200 ns and in presence of 150 mM NaCl (Figure 8, dotted blue and dotted brown curves), CPR adopted mainly two types of conformations: one with a sharp distribution centred at 20 ± 3 Å, and a second with a broad distribution of FMNH•/K668 distances between 60 and 100 Å. These two distinct families of conformations could be associated to the "locked/closed" and "unlocked/open" states, respectively. The sharp distribution obtained by MD confirmed that the distance distribution width of the DEER data probably arose mainly from conformational states of CPR than from rotamers of the label. In absence of salt (red and green curves), shorter FMNH•/K668 distances were observed. Two groups of preferred distances (around 10 and 20 Å) clearly stand out in the region corresponding to the "locked/closed" state. The small variation in distance in this conformation might be explained by the presence of numerous salt bridges and bonds that restrict interdomain movement. Two less populated groups appeared at 32 and 60 Å, representing a significant part of the conformational landscape of the protein when starting from an open conformation.

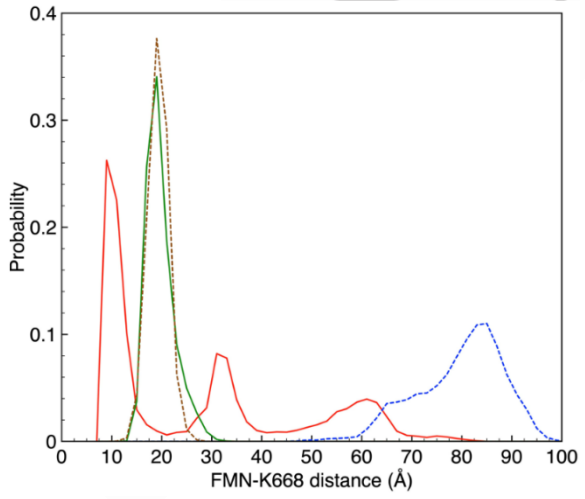

Figure 8. FMNH•/K668 distance distribution for CPR in the FAD/FMNH• redox state using the data for the last 200 ns. Starting point of the simulation corresponds to the "unlocked/open" conformation (no salt: red, 150mM NaCl: dotted blue) or "locked/closed" conformation (no salt: green, 150mM NaCl: dotted brown).

Overall, MD calculations were in agreement with our experimental results in showing the presence of two preferred "unlocked/open" or "locked/closed" conformations, the latter being stabilized whatever the ionic strength. On the other hand, the presence of salt seemed to promote an "unlocked/open" state, which existed in a range of several conformations. This flexibility on the open conformational states may be necessary to interact with several partners, in particular specific CYP isoforms and/or substrate binding.[10,47,53,54]

Conclusion

In this work, SDSL-EPR as well as MD were used to study a specific flavoprotein involved in electron transfer from NADPH to CYPs, *i.e.* CPR. Soluble Δ66-CPR, devoid of both linker truncation (known to impose a specific conformation on the system) and any other mutation, was employed for an unconstrained study of the protein in solution. We have succeeded in the insertion of the ncaa *p*AzPhe into either the FAD or FMN domain (positions 668 and 157, respectively). We then selectively and efficiently labelled the ncaa using the HO-4451 nitroxide spin label, through a SPAAC reaction, without modifying the protein activity.[19] Additionally, we prepared the FMNH• semiquinone state of the labelled protein in order to use the flavin site as an intrinsic spin centre, together with nitroxide spin HO-4451 label for distance measurements by DEER experiments. We demonstrated that the specific redox state FAD/FMNH• of CPR, the resting state, exists in solution as two major states, namely "unlocked/open" and "locked/closed". In the presence of high salt concentration, the two flavin domains moved significantly apart, resulting in a FAD to FMN domain distance consistent with an extensively "open" state in solution. This highly open electrostatic driven state was obtained for the one-electron reduced form of CPR, in contrast to other reported data for which CPR was prepared as fully oxidized or fully reduced protein.[6,51,55,56] Moreover, this extended "open" state is consistent with the possibility of the protein to experience a large scale conformational landscape, as shown by the chimeric crystal structure of *Saccharomyces cerevisiae*/*Homo sapiens* CPR construct.[9] This result is confirmed by MD simulations where "unlocked/open" state was shown to be stable as an ensemble of conformations over a range of 60 to 100 Å in presence of salt, over several hundreds of nanoseconds. In comparison with other biophysical studies, our results provide evidence for an ensemble of wider opening conformations of the one electron reduced CPR in solution than what was reported on oxidized or reduced CPR.[51]We also observed an increase of activity of soluble CPR as a function of salt concentration. In light of our DEER and MD results, this could be interpreted as a higher efficiency of the "open" state of CPR for ET to an external partner (cytochrome c or CYPs). In parallel, the "closed" state was shown to be stable but with a restricted scale of space. In the one-electron reduced state of human soluble CPR, ionic strength induces a switch from the "locked/closed" to the "unlocked/open" states. The range of conformations in the unlocked/open state may be crucial to the interaction and binding between CPR and CYPs, possibly via the selection of competent conformations depending on the redox

state of CPR. The alterations in the conformational equilibrium of CPR induced by mutations on the FD or by the binding of small molecules have been previously documented.[2,10] However, these studies did not concurrently track the redox state of flavins. To address this gap, the next phase will involve the monitoring of CPR's distance changes during the main redox states implicated in ET: FAD/FMN, FAD/FMNH•, and $FADH_2$/$FMNH_2$, and/or under varying ionic strengths. This will provide comprehensive insights into the dynamic interplay between locked/closed and unlocked/open CPR states at various redox states, particularly those competent in ET to CYPs. Our investigation marks a pioneering achievement by introducing a novel methodology, concurrently employing a flavin semiquinone and a nitroxide specific to ncaa, within a protein framework for DEER distance measurements. Notably, this innovative approach holds the potential for widespread applications across various flavoproteins, when the existence of non-modifiable cysteine residues is present, and when the stabilization of sq is feasible. We worked on the soluble CPR but this work has the potential to be applied to the full-length protein to study its native environment and its partnership with CYPs, by assessing the effect of membrane, the nature of lipids,[57–60] co-enzyme binding and redox chemistry in structural changes. Understanding the interplay between CPR and CYPs is of high importance due to their profound impact on drug and steroid metabolism.

Supporting Information

The authors have cited additional references within the Supporting Information.[61–78]

Acknowledgements

This work was supported by the Centre National de la Recherche Scientifique (CNRS) and Aix-Marseille Université (AMU). We are grateful to the EPR-MRS facilities of the Aix-Marseille EPR centre and acknowledge the financial support of the French research infrastructure INFRANALYTICS (FR2054). This project has received funding from the European Union's Horizon 2020 research and innovation programme under grant agreement No 101004806 MOSBRI-2021-28 and National Research, Development, and Innovation Fund of Hungary, NKFI K 137793. We thank Prof. Wayne Hubbell and Evan Brooks, from Jules Stein Eye Institute at UCLA, for helpful discussions on labelling reactions, Prof. Gunnar Jeschke, from ETH Zürich, for implementation of the HO-4451 label in MMM software. We thank AMU fellowship for M1 internship for Colette Maignet-Magard. The Centre de Calcul Intensif d'Aix-Marseille is acknowledged for granting access to its high-performance computing resources.

Keywords: Site Directed Spin Labelling EPR spectroscopy • Cytochrome P450 oxidoreductase • DEER • flavin • non canonical amino acid • Molecular Dynamic simulations

[1] J. Hakkola, J. Hukkanen, M. Turpeinen, O. Pelkonen, *Arch. Toxicol.* **2020**, *94*, 3671–3722.

[2] F. Esteves, P. Urban, J. Rueff, G. Truan, M. Kranendonk, *IJMS* **2020**, *21*, 6669.

[3] L. Aigrain, F. Fatemi, O. Frances, E. Lescop, G. Truan, *IJMS* **2012**, *13*, 15012–15041.

[4] D. Hamdane, C. Xia, S.-C. Im, H. Zhang, J.-J. P. Kim, L. Waskell, *J. Biol. Chem.* **2009**, *284*, 11374–11384.

[5] T. M. Hedison, S. Hay, N. S. Scrutton, *FEBS J* **2015**, *282*, 4357–4375.

[6] O. Frances, F. Fatemi, D. Pompon, E. Guittet, C. Sizun, J. Pérez, E. Lescop, G. Truan, *Biophysical Journal* **2015**, *108*, 1527–1536.

[7] R. B. Quast, F. Fatemi, M. Kranendonk, E. Margeat, G. Truan, *ChemBioChem* **2019**, *20*, 659–666.

[8] T. M. Hedison, N. S. Scrutton, *FEBS J* **2019**, *286*, 2004–2017.

[9] L. Aigrain, D. Pompon, S. Moréra, G. Truan, *EMBO Rep* **2009**, *10*, 742–747.

[10] F. Esteves, C. M. M. Almeida, S. Silva, I. Saldanha, P. Urban, J. Rueff, D. Pompon, G. Truan, M. Kranendonk, *Biomolecules* **2023**, *13*, 1083.

[11] C. Altenbach, C. J. López, K. Hideg, W. L. Hubbell, in *Methods in Enzymology*, Elsevier, **2015**, pp. 59–100.

[12] J. P. Klare, *Protein Interactions* **2017**, 22.

[13] M. Martinho, E. Fournier, N. Le Breton, E. Mileo, V. Belle, in *Electron Paramagnetic Resonance* (Eds.: V. Chechik, D.M. Murphy), Royal Society Of Chemistry, Cambridge, **2018**, pp. 66–88.

[14] M. Pannier, S. Veit, A. Godt, G. Jeschke, H. W. Spiess, *J. Magn. Reson.* **2011**, *213*, 316–325.

[15] E. Fournier, S. Tachon, N. J. Fowler, G. Gerbaud, P. Mansuelle, P. Dorlet, S. P. Visser, V. Belle, A. J. Simaan, M. Martinho, *Chem. Eur. J.* **2019**, *25*, 13766–13776.

[16] A. L. Shen, D. S. Sem, C. B. Kasper, *Journal of Biological Chemistry* **1999**, *274*, 5391–5398.

[17] C. Xia, A. L. Shen, P. Duangkaew, R. Kotewong, P. Rongnoparut, J. Feix, J.-J. P. Kim, *Biochemistry* **2019**, *58*, 2408–2418.

[18] M. R. Fleissner, E. M. Brustad, T. Kalai, C. Altenbach, D. Cascio, F. B. Peters, K. Hideg, S. Peuker, P. G. Schultz, W. L. Hubbell, *Proceedings of the National Academy of Sciences* **2009**, *106*, 21637–21642.
[19] T. Kálai, M. R. Fleissner, J. Jekő, W. L. Hubbell, K. Hideg, *Tetrahedron Letters* **2011**, *52*, 2747–2749.
[20] P. Widder, F. Berner, D. Summerer, M. Drescher, *ACS Chem. Biol.* **2019**, *14*, 839–844.
[21] A. Kugele, S. Ketter, B. Silkenath, V. Wittmann, B. Joseph, M. Drescher, *Chem. Commun.* **2021**, *57*, 12980–12983.
[22] M. A. Shandell, Z. Tan, V. W. Cornish, *Biochemistry* **2021**, *60*, 3455–3469.
[23] K. Lang, J. W. Chin, *Chem. Rev.* **2014**, *114*, 4764–4806.
[24] M. J. Schmidt, A. Fedoseev, D. Summerer, M. Drescher, in *Methods in Enzymology*, Elsevier, **2015**, pp. 483–502.
[25] S. Jana, E. G. B. Evans, H. S. Jang, S. Zhang, H. Zhang, A. Rajca, S. E. Gordon, W. N. Zagotta, S. Stoll, R. A. Mehl, *J. Am. Chem. Soc.* **2023**, *145*, 14608–14620.
[26] S. Ketter, B. Joseph, *J. Am. Chem. Soc.* **2023**, *145*, 960–966.
[27] G. Gerbaud, B. Barbat, M. Tribout, E. Etienne, V. Belle, B. Douzi, R. Voulhoux, A. Bonucci, *ChemBioChem* **2023**, *24*, e202300099.
[28] K. Singewald, X. Bogetti, K. Sinha, G. S. Rule, S. Saxena, *Angew. Chem. Int. Ed.* **2020**, *59*, 23040–23044.
[29] A. Giannoulis, Y. Ben-Ishay, D. Goldfarb, *Methods Enzymol* **2021**, *651*, 235–290.
[30] L. Galazzo, E. Bordignon, *Prog. Nucl. Magn. Reson. Spectrosc.* **2023**, *134–135*, 1–19.
[31] D. Nohr, R. Rodriguez, S. Weber, E. Schleicher, *Front. Mol. Biosci.* **2015**, *2*, DOI 10.3389/fmolb.2015.00049.
[32] D. Nohr, S. Weber, E. Schleicher, in *Methods in Enzymology*, Elsevier, **2019**, pp. 251–275.
[33] C. W. M. Kay, C. Elsässer, R. Bittl, S. R. Farrell, C. Thorpe, *J. Am. Chem. Soc.* **2006**, *128*, 76–77.
[34] S. Hay, S. Brenner, B. Khara, A. M. Quinn, S. E. J. Rigby, N. S. Scrutton, *J. Am. Chem. Soc.* **2010**, *132*, 9738–9745.
[35] A. Sobolewska-Stawiarz, N. G. H. Leferink, K. Fisher, D. J. Heyes, S. Hay, S. E. J. Rigby, N. S. Scrutton, *J. Biol. Chem.* **2014**, *289*, 11725–11738.
[36] D. Samanta, J. Widom, P. P. Borbat, J. H. Freed, B. R. Crane, *J. Biol. Chem.* **2016**, *291*, 25809–25814.
[37] I. V. Borovykh, S. Ceola, P. Gajula, P. Gast, H.-J. Steinhoff, M. Huber, *Journal of Magnetic Resonance* **2006**, *180*, 178–185.
[38] M. A. Swanson, V. Kathirvelu, T. Majtan, F. E. Frerman, G. R. Eaton, S. S. Eaton, *J. Am. Chem. Soc.* **2009**, *131*, 15978–15979.
[39] S. Kucher, S. Korneev, S. Tyagi, R. Apfelbaum, D. Grohmann, E. A. Lemke, J. P. Klare, H.-J. Steinhoff, D. Klose, *Journal of Magnetic Resonance* **2017**, *275*, 38–45.
[40] T. Braun, M. Drescher, D. Summerer, *IJMS* **2019**, *20*, 373.
[41] D. S. Sem, C. B. Kasper, *Biochemistry* **1993**, *32*, 11539–11547.
[42] M. Martinho, J. Habchi, Z. El Habre, L. Nesme, B. Guigliarelli, V. Belle, S. Longhi, *Journal of Biomolecular Structure and Dynamics* **2013**, *31*, 453–471.
[43] V. Belle, S. Rouger, S. Costanzo, S. Longhi, A. Fournel, in *Instrumental Analysis of Intrinsically Disordered Proteins*, **2010**, pp. 131–169.
[44] J. L. Vermilion, M. J. Coon, *Journal of Biological Chemistry* **1978**, *253*, 8812–8819.
[45] J. L. Vermilion, M. J. Coon, *Journal of Biological Chemistry* **1978**, *253*, 2694–2704.
[46] S. Brenner, S. Hay, A. W. Munro, N. S. Scrutton, *FEBS Journal* **2008**, *275*, 4540–4557.
[47] D. Campelo, T. Lautier, P. Urban, F. Esteves, S. Bozonnet, G. Truan, M. Kranendonk, *Front. Pharmacol.* **2017**, *8*, 755.
[48] Y. Polyhach, E. Bordignon, G. Jeschke, *Phys. Chem. Chem. Phys.* **2011**, *13*, 2356–2366.
[49] L. Fábregas Ibáñez, G. Jeschke, S. Stoll, *Magn Reson (Gott)* **2020**, *1*, 209–224.

[50] L. Fábregas-Ibáñez, M. H. Tessmer, G. Jeschke, S. Stoll, *Phys. Chem. Chem. Phys.* **2022**, *24*, 2504–2520.
[51] J. Ellis, A. Gutierrez, I. L. Barsukov, W.-C. Huang, J. G. Grossmann, G. C. K. Roberts, *Journal of Biological Chemistry* **2009**, *284*, 36628–36637.
[52] M. Iijima, J. Ohnuki, T. Sato, M. Sugishima, M. Takano, *Sci. Rep.* **2019**, *9*, 9341.
[53] M. Šrejber, V. Navrátilová, M. Paloncýová, V. Bazgier, K. Berka, P. Anzenbacher, M. Otyepka, *J. Inorg. Biochem.* **2018**, *183*, 117–136.
[54] S. D. Burris-Hiday, E. E. Scott, *Journal of Biological Chemistry* **2023**, *299*, 105112.
[55] M. Wadsäter, T. Laursen, A. Singha, N. S. Hatzakis, D. Stamou, R. Barker, K. Mortensen, R. Feidenhans'l, B. L. Møller, M. Cárdenas, *Journal of Biological Chemistry* **2012**, *287*, 34596–34603.
[56] M. Jenner, J. Ellis, W. Huang, E. Lloyd Raven, G. C. K. Roberts, N. J. Oldham, *Angew. Chem. Int. Ed.* **2011**, *50*, 8291–8294.
[57] K. Yamamoto, U. H. N. Dürr, J. Xu, S.-C. Im, L. Waskell, A. Ramamoorthy, *Sci Rep* **2013**, *3*, 2538.
[58] R. Huang, K. Yamamoto, M. Zhang, N. Popovych, I. Hung, S.-C. Im, Z. Gan, L. Waskell, A. Ramamoorthy, *Biophysical Journal* **2014**, *106*, 2126–2133.
[59] K. A. Gentry, G. M. Anantharamaiah, A. Ramamoorthy, *Chem. Commun.* **2019**, *55*, 13422–13425.
[60] C. Barnaba, E. Taylor, J. A. Brozik, *J. Am. Chem. Soc.* **2017**, *139*, 17923–17934.
[61] N. J. Agard, J. A. Prescher, C. R. Bertozzi, *J. Am. Chem. Soc.* **2004**, *126*, 15046–15047.
[62] G. Jeschke, A. Bender, H. Paulsen, H. Zimmermann, A. Godt, *J. Magn. Reson.* **2004**, *169*, 1–12.
[63] B. Webb, A. Sali, *Curr. Protoc. Bioinform.* **2016**, *54*, 5.6.1-5.6.37.
[64] M. A. Martí-Renom, A. C. Stuart, A. Fiser, R. Sánchez, F. Melo, A. Sali, *Annu. Rev. Biophys. Biomol. Struct.* **2000**, *29*, 291–325.
[65] M. H. M. Olsson, C. R. Søndergaard, M. Rostkowski, J. H. Jensen, *J. Chem. Theory Comput.* **2011**, *7*, 525–537.
[66] W. L. Jorgensen, J. Chandrasekhar, J. D. Madura, R. W. Impey, M. L. Klein, *The Journal of Chemical Physics* **1983**, *79*, 926–935.
[67] J. Huang, S. Rauscher, G. Nawrocki, T. Ran, M. Feig, B. L. de Groot, H. Grubmüller, A. D. J. MacKerell, *Nat. Methods* **2017**, *14*, 71–73.
[68] A. Aleksandrov, *J. Comput. Chem.* **2019**, *40*, 2834–2842.
[69] E. Lindahl, B. Hess, D. van der Spoel, *Mol. Mod. Annual* **2001**, *7*, 306–317.
[70] D. Van Der Spoel, E. Lindahl, B. Hess, G. Groenhof, A. E. Mark, H. J. C. Berendsen, *Journal of Computational Chemistry* **2005**, *26*, 1701–1718.
[71] B. Hess, C. Kutzner, D. van der Spoel, E. Lindahl, *J. Chem. Theory Comput.* **2008**, *4*, 435–447.
[72] S. Pronk, S. Páll, R. Schulz, P. Larsson, P. Bjelkmar, R. Apostolov, M. R. Shirts, J. C. Smith, P. M. Kasson, D. van der Spoel, B. Hess, E. Lindahl, *Bioinformatics* **2013**, *29*, 845–854.
[73] M. J. Abraham, T. Murtola, R. Schulz, S. Páll, J. C. Smith, B. Hess, E. Lindahl, *SoftwareX* **2015**, *1–2*, 19–25.
[74] U. Essmann, L. Perera, M. L. Berkowitz, T. Darden, H. Lee, L. G. Pedersen, *The Journal of Chemical Physics* **1995**, *103*, 8577–8593.
[75] B. Hess, H. Bekker, H. J. C. Berendsen, J. G. E. M. Fraaije, *J. Comput. Chem.* **1997**, *18*, 1463–1472.
[76] S. Miyamoto, P. A. Kollman, *J. Comput. Chem.* **1992**, *13*, 952–962.
[77] G. Bussi, D. Donadio, M. Parrinello, *The Journal of Chemical Physics* **2007**, *126*, 014101.
[78] M. Parrinello, A. Rahman, *Journal of Applied Physics* **1981**, *52*, 7182–7190.

Entry for the Table of Contents

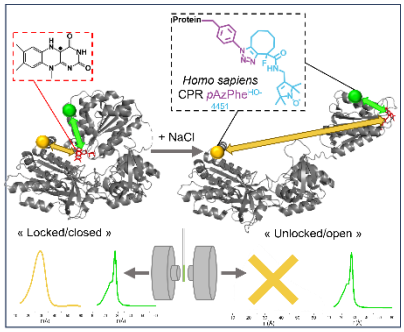

Exploring dynamics is crucial for understanding Cytochrome P450 Reductase's electron transfer pathway. We innovatively studied its one-electron-reduced state using non-canonical amino acid and a semi-reduced flavin. This novel approach enabled distance measurement by Double Electron Electron Resonance on this specific redox state for the first time. Together with Molecular Dynamics studies, we showed the existence of an ensemble of conformations for the "open" state of the protein.

Institute and/or researcher Twitter usernames: @MartinhoMarlene